JOURNAL OF MATERIALS SCIENCE: MATERIALS IN MEDICINE **16** (2005) 1179– 1184

Effects of TiO_2, ZrO_2 and Al_2O_3 dopants on the compressive strength of tricalcium phosphate

Y. I. ZAWAHREH*, N. POPOVA, R. W. SMITH
Department of Mechanical and Materials Engineering, Queen's University, Nicol Hall, 60 Union Street, Kingston, Ontario, K7L 3N6, Canada
E-mail: yousef@zawahreh.com

J. HENDRY, T. J. N. SMITH
Millenium Biologix Corporation, 785 Midpark Drive, Kingston, Ontario, K7M 7G3, Canada

T. L. ZIOLO
EBI, L.P., 100 Interpace Parkway, Parsippany, NJ 07054, USA

Tricalcium phosphate (TCP) powders synthesised using the $Ca(NO_3)_2$ and $Ca(OH)_2$ routes were doped with TiO_2, ZrO_2 and Al_2O_3 in order to increase their compressive strength. An ultimate compressive strength (UCS) of 255 $\pm$ 6 MPa was achieved for approximately 10 vol% TiO_2 doping compared to 30 $\pm$ 3 MPa for an un-doped control processed and tested in the same manner. Higher levels of TiO_2 doping resulted in smaller increases in UCS with 30 and 50 vol% achieving 213 $\pm$ 9 and 178 $\pm$ 15 MPa, respectively. Very small amounts of Al_2O_3 doping ($<$0.5 vol%) also resulted in a stronger materials. However, under the processing conditions employed, higher levels of Al_2O_3 and ZrO_2 doping resulted in no beneficial effect on the UCS. Polyvinyl alcohol (PVA) was used as binding agent to facilitate processing. As expected, higher levels of PVA were associated with smaller increases in UCS. Powders synthesised using the $Ca(OH)_2$ route had smaller particle size and resulted in larger increases in UCS compared to the $Ca(NO_3)_2$-synthesised powders.

Although some powders contained α and β-TCP phases, no other calcium phosphate, CaO, $CaTiO_3$ or $CaZrO_3$ phases were detected. In conclusion, a significant increase in the UCS of TCP was achieved by doping with approximately 10 vol% TiO_2 which is expected to have little or no effect on the bioactivity or bioresorbability of the material.

1. Introduction

Many attempts have been made to strengthen hydroxyapatite bioceramics with metal oxide additions [1–6]. High strength, bioinert oxides such as TiO_2, Al_2O_3 [7] and cubic ZrO_2 are obvious candidates. Generally, low levels of doping result in significant increases in strength. However, higher levels of doping do not yield the expected higher strength values due to adverse effects on the sintering of the hydroxyapatite matrix [2], or decomposition of the latter into tricalcium phosphate (TCP) and $CaZrO_3$ [2, 3] or $CaTiO_3$ [8, 9] depending on the dopant used.

To date, no work is published on the strengthening of single-phase bioresorbable ceramics, specifically TCP. This paper investigates the effect of ZrO_2, TiO_2 and Al_2O_3 doping on the compressive strength of TCP. The doping levels were similar to those used in the Japanese Patent No. 1-111763 [1]. However, the processing procedure was different. Our long-term objective is to produce a strengthened resorbable material that can be used in load-bearing applications.

2. Methods and materials

2.1. Powder syntheses

Calcium-deficient apatite [reactant Ca/P = 1.665] was precipitated from solutions of $(NH_4)_2HPO_4$ and $Ca(NO_3)_2$ made basic by the addition of NH_4OH. The $Ca(OH)_2$ and H_3PO_4 reaction was also used to synthesise selected powders. In this case a reactant Ca/P ratio of 1.5 was used and no NH_4OH was added. In either case the dopants [$ZrO(NO_3)_2$, TiO_2 and Al_2O_3] were added to the reaction mixture which was then stirred for 1 h prior to filtration and subsequent drying overnight at 80 °C. The crushed powders were calcined at 900 °C for 1 h then milled for 1 h, using an alumina milling pot and media, before sieving through a 212 μm sieve.

*Author to whom all correspondence should be addressed.

TABLE I Approximate volume fraction composition of each powder tested and corresponding mole fraction calculated from the amount of reactants used

	Approx. volume %				Mole %			
	TCP	ZrO_2	TiO_2	Al_2O_3	TCP	ZrO_2	TiO_2	Al_2O_3
10Ti	90		10		66.3		33.7	
30Ti	70		30		33.4		66.6	
50Ti	50		50		17.6		82.4	
40Zr-10Ti	50	40	10		15.6	70.1	14.4	
10Zr-40Ti	50	10	40		17.2	19.3	63.5	
0.5Zr-49.5Ti	50	0.5	49.5		17.8	1.0	81.2	
10Al	90			10	24.8			75.2
30Al	70			30	8.0			92.0
50Al	50			50	3.6			96.4
0.5Al	99.5			0.5	93.6			6.4
40Zr-10Al	50	40		10	12.1	54.4		33.5
10Zr-40Al	50	10		40	7.2	13.6		79.2

The approximate volume percentages of dopants and the calculated mole percentages (from mass of reactants) are given in Table I. Powders synthesised using the $Ca(NO_3)_2$ route are denoted with the prefix *n*-while $Ca(OH)_2$ powders are prefixed with *h*-.

2.2. Compression testing

Compression test pieces were made by pressing the sieved powders in a 6 mm diameter steel die under ∼120 MPa. The cylindrical specimens used had length to diameter ratios in the range 1.9–2.1 in accordance with ASTM C1424-99 [10]. A polyvinyl alcohol (PVA) binding agent (2.5 wt%) was used. The green compacts were heated at 550 °C for 1 h then sintered at 1175 °C for 1 h and cooled to room temperature at 5 °C. min^{-1}. Uniaxial compression tests were performed on 5 samples for each composition using a strain rate of 3×10^{-3} s^{-1}. A PVA solution of 7.5 wt% was also used as binding agent for 10 other specimens from selected n- and h- compositions.

2.3. Characterisation

Phase composition of these powders was determined using Co $K\alpha_{1+2}$ X-ray diffraction (X'pert Pro and an X'celerator detector, Philips). Scans were obtained between 10–80 ° 2θ using the equivalent of a 0.02 ° step size and 50 s exposure time. Peaks were identified using ICDD powder diffraction data cards [11].

After sintering, the apparent density of each specimen was measured and the percentage densification calculated. Theoretical bulk densities of 2.86, 3.07, 4.26, 5.83 and 3.97 g·cm^{-3} were used for α-TCP, β-TCP, TiO_2, ZrO_2 and Al_2O_3, respectively. The approximate volume percentages were used for the dopants whilst that of the TCP phase was determined from XRD analysis.

3. Results and discussion

3.1. Mechanical and physical properties

The ultimate compressive strength (UCS) of each composition is listed in Table II.The average density, the percentage densification and the median particle size are also given. Under these processing conditions (2.5% PVA binder; 1175 °C sintering), TiO_2 doping increased significantly the UCS of the ceramic as compared with an un-doped control sample processed and tested in the same manner, Fig. 1. Very small amounts of Al_2O_3

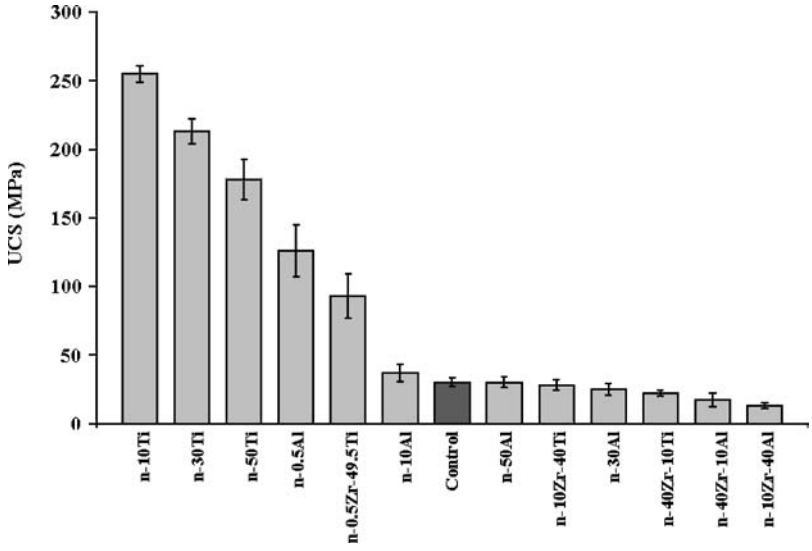

Figure 1 UCS of the $Ca(NO_3)_2$-synthesised powders using 2.5% PVA as binder compared to an un-doped control.

TABLE II UCS, density calculations (2.5% PVA as binder) and median particle size ($D_{0.5}$) for the $Ca(NO_3)_2$-synthesised powders

	UCS (MPa)	Density ($g \cdot cm^{-3}$)	Densification (%)	$D_{0.5}$ (μm)
n-10Ti	255 (6)	2.72	91	9.5
n-30Ti	213 (9)	2.42	74	3.8
n-50Ti	178 (15)	2.14	58	2.6
n-0.5Al	126 (19)	2.42	85	6.4
n-0.5Zr-49.5Ti	93 (16)	1.99	54	2.1
n-10Al	37 (6)	1.50	48	8.9
n-50Al	30 (4)	1.53	45	4.2
n-10Zr-40Ti	28 (4)	1.80	47	7.9
n-30Al	25 (4)	1.48	46	10.8
n-40Zr-10Ti	22 (2)	2.27	54	16.2
n-40Zr-10Al	17 (5)	1.86	44	6
n-10Zr-40Al	13 (2)	1.47	40	4.4

doping (<0.5 vol%) increased the compressive strength whilst higher levels did not. ZrO_2 doping decreased the compressive strength. With the exception of the *n*-50Ti specimens, the compositions that achieved densities over 74% of their theoretical bulk value exhibited the most significant increases in UCS. Indeed the higher the TiO_2 content, the lower the measured densification. No discernable effect on the UCS was observed for particle size. For instance, the ZrO_2-doped powders had small median particle sizes and bimodal size distributions yet their UCS was lower than the control.

The measurements obtained for the higher UCS compositions (*n*-10Ti, *n*-30Ti, *n*-50Ti, *n*-0.5Al and *n*-0.5Zr-49.5Ti) using 7.5% PVA binding agent are given in Table III and illustrated in Fig. 2.The anticipated reduction in the UCS compared with the 2.5% PVA specimens (Table I) ranged from 40 to 60%. The densification remained relatively constant with the exception of *n*-10Ti which had a 13% decrease.

The UCS measurements, densities, percentage densification and median particle size for the three compositions 10Ti, 30Ti and 0.5Al, synthesised via the $Ca(OH)_2$ route are given in Table IV.Although processed using the same conditions, these specimens had on average 75–80% higher UCS's and had densified more than their counterparts synthesised using the $Ca(NO_3)_2$ route (Table III). This is most likely due to the smaller particle sizes of these powders.

TABLE III UCS and density calculations (7.5% PVA as binder) for the higher strength $Ca(NO_3)_2$-synthesised powders

	UCS (MPa)	Density ($g \cdot cm^{-3}$)	Densification (%)
n-10Ti	153 (17)	2.34	78
n-30Ti	137 (17)	2.35	72
n-0.5Al	119 (18)	2.41	84
n-50Ti	71 (16)	2.18	59
n-0.5Zr-49.5Ti	70 (11)	2.24	61

TABLE IV UCS, density calculations (7.5% PVA as binder) and median particle size ($D_{0.5}$) for the higher strength $Ca(OH)_2$-synthesised powders

	UCS (MPa)	Density ($g \cdot cm^{-3}$)	Densification (%)	$D_{0.5}$ (μm)
h-10Ti	192 (19)	2.98	93	1.1
h-30Ti	174 (27)	2.60	76	1.1
h-0.5Al	161 (20)	2.87	94	1.4

TABLE V The calcium phosphate phase composition of each powder after calcination at 1175 °C calculated using the RIR method

	$Ca(NO_3)_2$ route		$Ca(OH)_2$ route	
	α-TCP (%)	β-TCP (%)	α-TCP (%)	β-TCP (%)
10Ti	92	8		100
30Ti	100			100
50Ti		100		
40Zr-10Ti	87	13	51	49
10Zr-40Ti	32	68	63	37
0.5Zr-49.5Ti		100		
10Al		100		
30Al	100			
50Al	100			
0.5Al	100			100
40Zr-10Al		100	100	
10Zr-40Al	55	45	100	

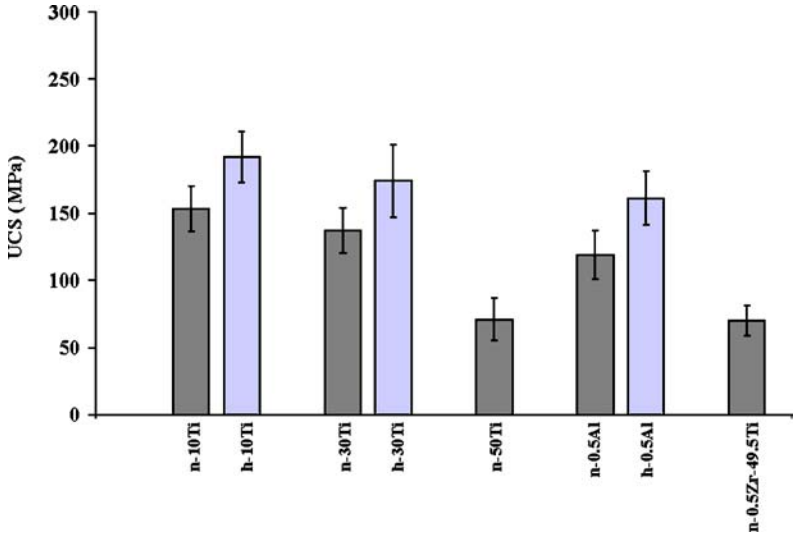

Figure 2 UCS of the high strength $Ca(NO_3)_2$- and $Ca(OH)_2$-synthesised powders using 7.5% PVA as binder.

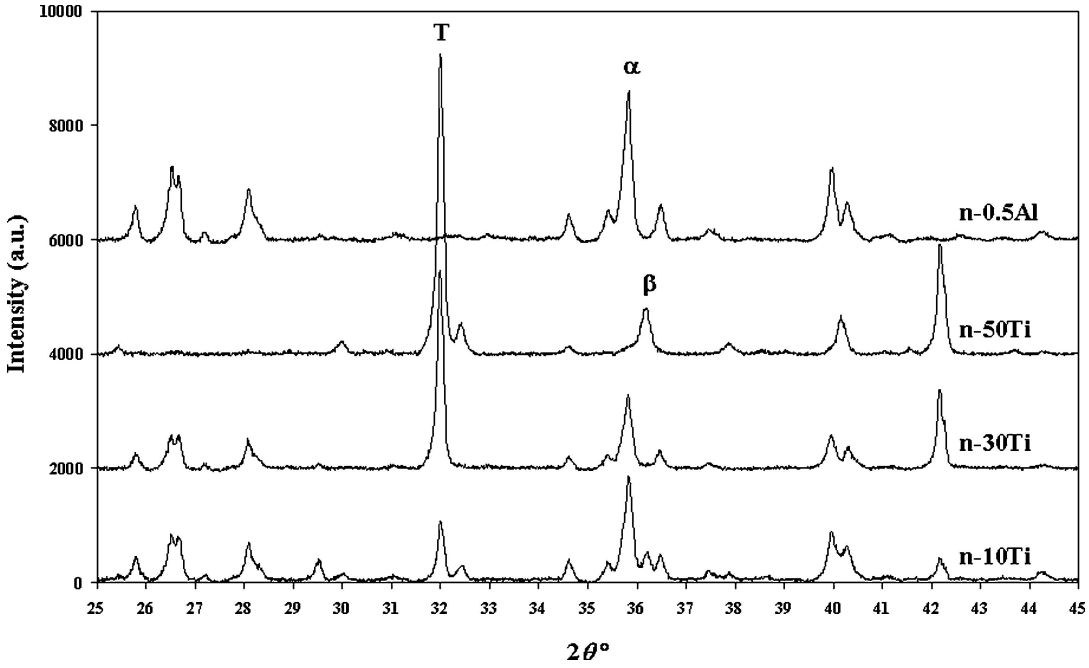

Figure 3 Co *Kα* XRD patterns of the high strength $Ca(NO_3)_2$-synthesised powders. α, β and T denote the 100% peaks for α-TCP, β-TCP and TiO_2, respectively. All unlabelled peaks correspond to a labelled phase.

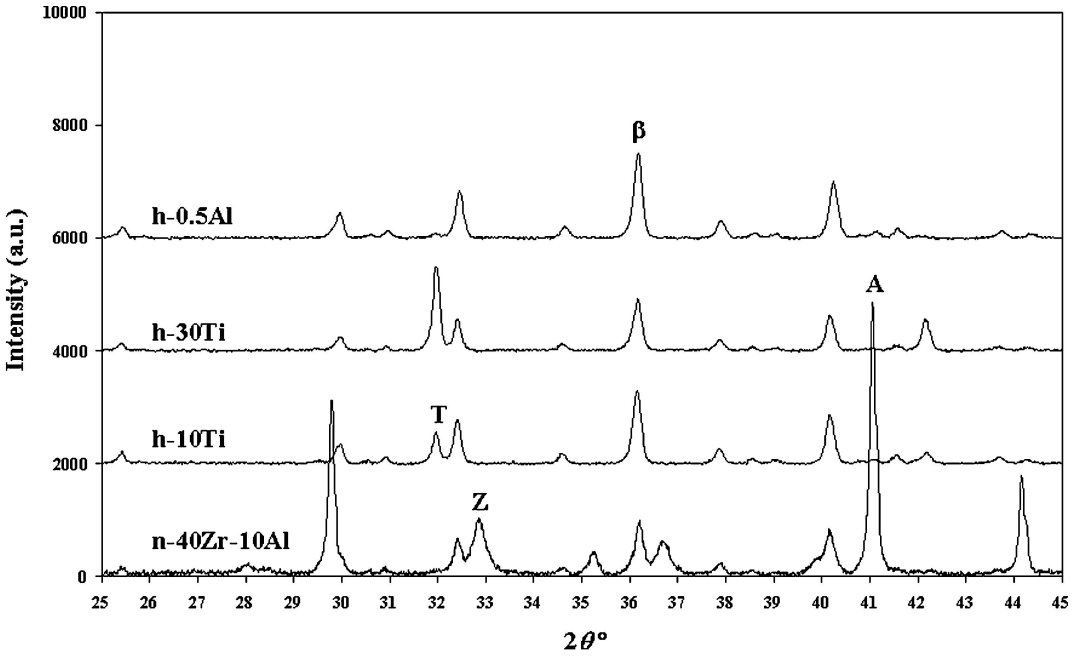

Figure 4 Co *Kα* XRD patterns of the high strength $Ca(OH)_2$-synthesised powders and a weak $Ca(NO_3)_2$-synthesised powder (*n*-40Zr–10Al). β, T, Z and A denote the 100% peaks for β-TCP, TiO_2, ZrO_2 and Al_2O_3, respectively. All unlabelled peaks correspond to a labelled phase.

3.2. X-ray diffraction (XRD)

Since the mass absorption coefficients of α- and β-TCP are the same, the normalised relative intensity ratio method (RIR) was used to determine the quantity of each of these phases in each powder composition from the respective 100% intensity peaks, Table V.No hydroxyapatite, tetracalcium phosphate, or CaO phases were present in any of the compositions. In contrast with previous work [2–4, 9, 12], no $CaZrO_3$ phase was present in the ZrO_2-doped powders nor was there a $CaTiO_3$ phase present in the TiO_2-doped powders. Rutile was the TiO_2 phase present in the TiO_2-doped powders. Further, the ZrO_2 phase comprised the weaker monoclinic baddeleyite polymorph. This was to be expected for the sintering regime employed and since no stabilising agents were added.

As illustrated in Fig. 3,TiO_2 doping of the $Ca(NO_3)_2$ route stabilised α-TCP at the 10 and 30 vol% levels while 50 vol% gave rise to β-TCP. In contrast, the calcium phosphate phase resulting from 10 and 30 vol% TiO_2 doping of the $Ca(OH)_2$ route was β-TCP, Fig. 4.However, even though most Al_2O_3-doped powders gave rise to α-TCP, this did not increase the UCS, particularly in the case of higher levels of doping (30 and 50 vol%). The double-doped pow-

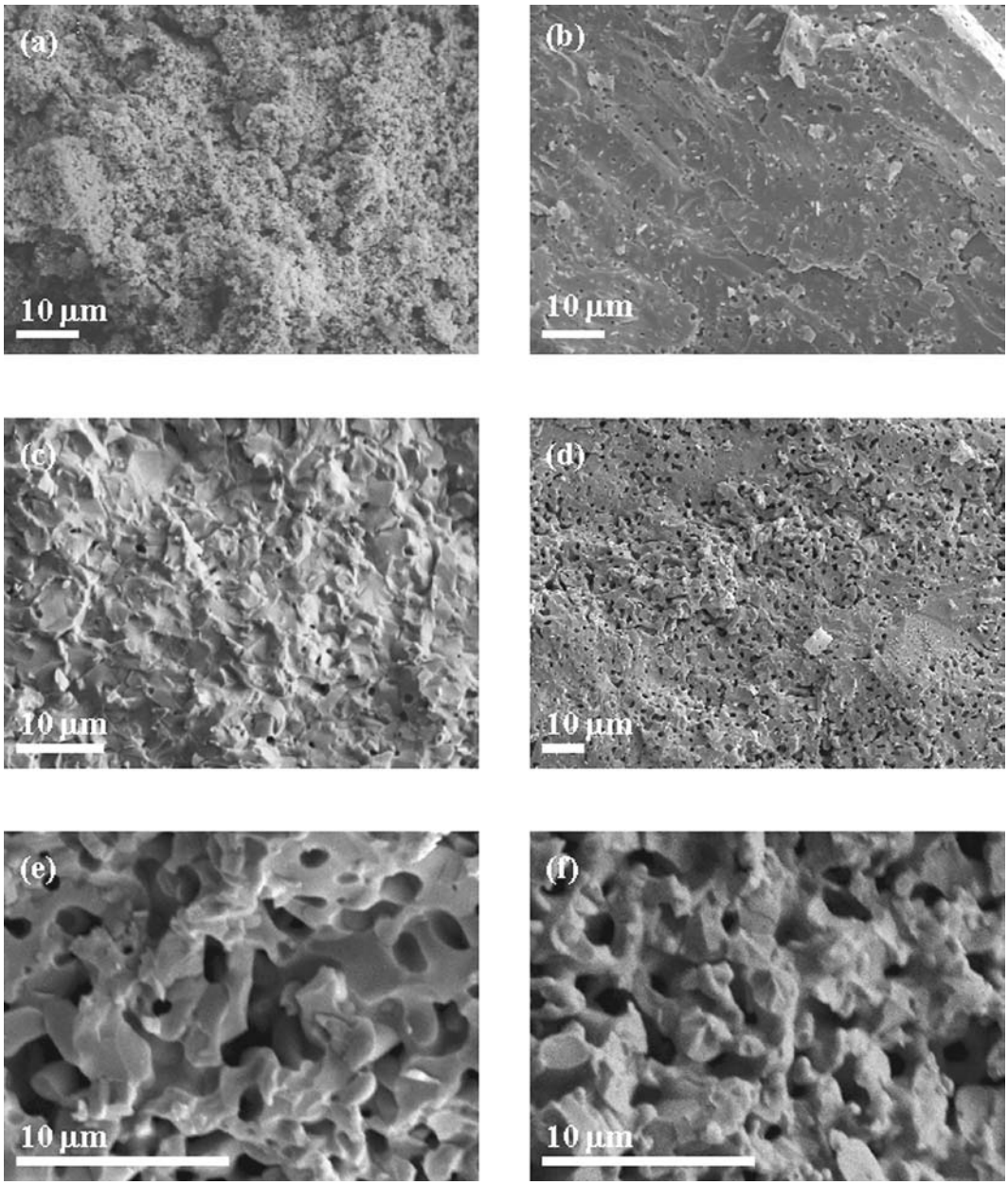

Figure 5 Fracture surface SEM micrographs: (a) *n*-40Zr-10Al [2.5% PVA], (b) *n*-10Ti [2.5% PVA], (c) *h*-10Ti [7.5% PVA], (d) *n*-10Ti [7.5% PVA], (e) *n*-30Ti [7.5% PVA] and (f) *h*-30Ti [7.5% PVA].

ders (40Zr-10Ti, 10Zr-40Ti, 40Zr-10Al and 10Zr-40Al) were found to be multiphasic with respect to the calcium phosphate present. This may have inhibited the sintering process resulting in their low UCS.

3.3. Scanning electron microscopy (SEM)

SEM of the fracture surfaces revealed that the weaker compositions had not sintered, Fig. 5(a).Despite the significant improvement in the compressive strength, residual microporosity still remained, as illustrated in Fig. 5(b)–(f). Pore size in the $Ca(NO_3)_2$-synthesised powders remained constant ($\sim$1–5 μm diameter) with PVA content. However, the number of pores and the level of interconnectivity increased with increasing PVA content, Fig. 5(b) and (d). The pores observed for the $Ca(OH)_2$-synthesised *h*-10Ti specimens (7.5% PVA), Fig. 5(c), were also similar in size to those of the 2.5% PVA *n*-10Ti, although the sample was less porous. These findings are in agreement with UCS and XRD data since *h*-10Ti is a β-TCP with a higher UCS than the α-TCP *n*-10Ti. Smaller, fewer pores and lower levels of interconnectivity were observed for *h*-10Ti compared with *n*-10Ti, Fig. 5(c) and (d). The smaller particle size of *h*-10Ti enhanced sintering resulting in a denser ceramic with a higher UCS. The morphologies of *n*-30Ti and *h*-30Ti were similar with *n*-30Ti having slightly larger pores which appear to be more interconnected, thus accounting for the lower UCS of *n*-30Ti, Fig. 5(e) and (f).

4. Conclusions

Under the processing conditions used, TiO_2 increased significantly the compressive strength of TCP and generally stabilised the α-polymorph. The increase in UCS value compared to an un-doped material was found to be inversely proportional to the vol% of TiO_2. This is a welcome result since a stronger material is achieved

at little or no cost to bioactivity or bioresorbability. As expected, UCS is inversely proportional to binder content whilst temperatures in excess of 1175 °C are required to sinter the Al_2O_3- and/or ZrO_2-doped TCP. The higher strength cubic or tetragonal ZrO_2 polymorphs were not stabilised under these conditions suggesting that there was no Ca^{2+} migration into the ZrO_2 lattice. Doped $Ca(OH)_2$-synthesised powders had smaller median particle sizes which enhanced sintering and resulted in higher values for UCS compared to those of the $Ca(NO_3)_2$-synthesised powders.

Acknowledgments

The financial support of MMO/CRESTech (Canada) and Millenium Biologix Corp. is gratefully acknowledged.

References

1. T. SUZUKI, K. KADOYA, S. HARADA, K. K. NIKKI and Y. ITO, J P Pat. No. 1-111763 (1989).
2. J. A. DELGADO, S. MARTINEZ, M. P. GINEBRA, L. MOREJON, N. CARLSSON, E. FERNANDEZ, J. A. PLANELL, M. T. CLAVAGUERA-MORA and J. RODRIGUEZ-VIEJO, in Proc. of the 13th Int. Symp. On Ceramics in Medicine, Bologna, Italy, November 2000 (Trans Tech Publications, Switzerland, 2001) p. 151.
3. Y. -M. KONG, H. -E. KIM and I. -S. LEE, in Proc. of the 6th World Biomaterials Congress Transactions, Kamuela, HI, USA, (Society for Biomaterials, Mt. Laurel, NJ, USA, 2000) 432.
4. M. R. TOWLER and I. R. GIBSON, *J. Mater. Sci. Lett.* **20** (2001) 1719.
5. J. LI, L. HERMANSSON and R. SÖREMARK, *J. Mater. Sci.: Mater. In Med.* **4** (1993) 50.
6. M. TAKAGI, M. MOCHIDA, N. UCHIDA, K. SAITO and K. UEMATSU, *ibid.* **3** (1992) 199.
7. S. F. HULBERT, J. S. MORRISON and J. J. KLAWITTER, *J. Biomed. Mater. Res.* **6** (1972) 347.
8. J. WENG, X. LIU, X. ZHANG and X. JI, *J. Mater. Sci. Lett.* **13** (1994) 157.
9. I. MANJUBALA and T. S. SAMPATH-KUMAR, *Biomater.* **21** (2000) 1995.
10. ASTM C1424-99, in "Annual Book of ASTM Standards" (ASTM International, West Conshohocken, PA, USA, 1999) 664.
11. PDF Cards, International Committee for Diffraction Data (ICDD), Newton Square, Pennsylvania, PA, USA.
12. J.-M. WU and T.-S. YEH, *J. Mater. Sci.* **23** (1988) 3771.

Received 30 June
and accepted 19 August 2005